Bithermal Low-Cycle Fatigue Evaluation of Automotive Exhaust System Alloy SS409

Gui-Ying Lu[1] and Mike B. Behling
Arvin Exhaust Systems
1531 13th Street, Columbus, IN 47201

Gary R. Halford
NASA-Glenn Research Center
21000 Brookpark Road, Cleveland, OH 44135

Abstract

This investigation provides, for the first time, cyclic strainrange-controlled, thermomechanical fatigue results for the ferritic stainless steel alloy SS409. The alloy has seen extensive application for automotive exhaust system components. The data were generated to calibrate the Total Strain Version of the Strainrange Partitioning (TS-SRP) method for eventual application to the design and durability assessment of automotive exhaust systems. The thermomechanical cyclic lifetime and cyclic stress-strain constitutive behavior for alloy SS409 were measured using bithermal tests cycling between isothermal extremes of 400 and 800°C. Lives ranged up to 10,000 cycles to failure with hold-times of 0.33 to 2.0 minutes. The bithermal fatigue behavior is compared to isothermal, strain-controlled fatigue behavior at both 400 and 800°C. Thermomechanical cycling was found to have a profound detrimental influence on the fatigue failure resistance of SS409 compared to isothermal cycling. Supplementary bithermal

[1] Whom correspondence should be addressed to. Currently with General Motors Technical Centers, VSAS Global Process Center, Mail Code 480-305-200, 6440 E. 12 Mile Road, Warren, MI 48090-9000

cyclic stress-strain constitutive tests with hold-times ranging from 40 seconds up to 1.5 hours were conducted to calibrate the TS-SRP equation for extrapolation to longer lifetime predictions. Observed thermomechanical (bithermal) fatigue lives correlated well with lives calculated using the calibrated TS-SRP equations: 70% of the bithermal fatigue data fall within a factor of 1.2 of calculated life; 85% within a factor of 1.4; and 100% within a factor of 1.8.

[Key words: SS409, thermomechanical fatigue, low-cycle fatigue, bithermal fatigue, cyclic constitutive behavior, Strainrange Partitioning].

Nomenclature

A' general constant in empirical equations

B coefficient of general elastic strainrange versus life relation

B_{pp} coefficient of PP elastic strainrange versus life relation

C' coefficient of equivalent inelastic line for combined plastic-creep fatigue cycles

C_{pp} coefficient of PP inelastic strainrange versus pure PP fatigue life

C_{pc} coefficient of PC inelastic strainrange versus pure PC creep-fatigue life

b power of cyclic life for elastic strainrange versus life relation

c power of cyclic life for inelastic strainrange versus life relation

m general power of time in empirical constitutive equations

n cyclic strain-hardening exponent

δt hold-time per cycle

F_{pc} PC strainrange fraction, $\Delta\varepsilon_{pc}/\Delta\varepsilon_{in}$

F_{pp} PP strainrange fraction, $\Delta\varepsilon_{pp}/\Delta\varepsilon_{in}$

K_{pc} cyclic strain-strain ($\Delta\varepsilon_{el}$ vs. $\Delta\varepsilon_{in}$) coefficient for PC cycling

K_{pp} cyclic strain-strain ($\Delta\varepsilon_{el}$ vs. $\Delta\varepsilon_{in}$) coefficient for PP cycling

N_f fatigue life, cycles (number of cycles at 20% drop in tensile load from half-life cycle)

α general power of total strainrange in empirical constitutive equations

$\Delta\varepsilon_{el}$ elastic strainrange

$\Delta\varepsilon_{in}$ inelastic strainrange

$\Delta\varepsilon_{to}$ total strainrange

$\Delta\varepsilon_{pp}$ tensile plastic-compressive plastic component of inelastic strainrange

$\Delta\varepsilon_{pc}$ tensile plastic-compressive creep component of inelastic strainrange

I. Introduction

Automotive exhaust system designers are facing the challenges of emission control, durability, reliability, fuel efficiency and packaging density. Rising operating temperatures subject systems to severe thermal fatigue loading. More thermal fatigue cycles will be applied as warrantee periods are extended due to use of more corrosion/oxidation resistant alloys. Thermal fatigue life prediction thus becomes essential for addressing exhaust system durability requirements. Typical thermal cycles for exhaust system components are caused by transient engine operation that produces cyclic temperature gradients and hence cyclic strains. The temperature/strain relation is "out-of-phase", i. e. compression while hot, tension while cool. In addition, vibration created by road roughness and turning maneuvers imposes mechanical bending strains. Because of their high frequency, these mechanical strains are imposed isothermally. Since exhaust systems rapidly heat to operating temperatures, most mechanical fatigue occurs at relatively high temperatures. The fatigue damage due to vibration can be handled independently in the durability analysis of an exhaust system.

Viable TMF life prediction models typically are calibrated with data from experiments that simulate many of the critical features of service operation. Cyclic stress-strain-temperature-time response as well as cyclic crack initiation resistance is documented and used to evaluate lifing model constants. TMF characteristics are measured in this study using the bithermal testing techniques reported in Refs. [4,5]. Low-cycle TMF data were generated for the ferritic stainless steel exhaust system alloy, SS409. The TMF life prediction model of choice is the Total Strain Version of the Strainrange Partitioning (TS-SRP) [5,6]. This paper represents the first reported attempt to capture the thermomechanical fatigue resistance of SS409 by any high-temperature

life prediction method. Strainrange Partitioning is a high-temperature life prediction method based on the premise that fatigue life is a function of the relative magnitudes of cyclically imposed time-independent plasticity and time-dependent creep strains. Figure 1 illustrates the governing total strainrange versus life equation of the TS-SRP version [5-6] for the two most pertinent types of SRP cycles for the current application.

$$\Delta\varepsilon_{to} = B(N_f)^b + C'(N_f)^c \quad (1)$$

The relevant supporting equations are summarized in the figure. The reader is referred to Refs. [5-7] for details.

II. Material Characterization

Tensile, isothermal fatigue, bithermal fatigue, and continuous thermomechanical fatigue tests were conducted to better understand SS409 behavior. Table 1 lists the test types and temperatures used in this investigation. The following experimental details will focus on bithermal fatigue testing.

2.1 Material, Specimens, and Test Equipment

SS409-HP10 (nominal composition: 0.0147C-0.32Mn-0.022P-0.002S-0.10Si-10.81Cr-0.12Ni-0.08N-0.20Ti-0.03Al) used in this investigation was received from Armco, Inc. in the form of hot rolled and annealed (1725°C) plate about 0.630 thick. This grade of ferritic stainless steel is the most widely used in automotive exhaust systems today.

The bithermal fatigue testing was performed at Mar-Test Inc., Cincinnati, OH. Both the servo-hydraulic testing machine and the heating system were closed-loop computer controlled using custom software developed by McGaw Technologies, Lakewood, OH. Hourglass-shaped specimens (min. diameter of 0.312 in, radius of 1.0 in and overall length of 2.9 in) were heated by an induction heating system. Temperature was controlled and measured by thermocouples spot-welded midway between the minimum cross section and the end of the hourglass-shaped test section. The temperature of the minimum cross section was measured with a wrap-around thermocouple, which was removed before the start of the test. Strains were measured with a diametral extensometer positioned at the minimum cross section of the hourglass-shaped specimen. The tensile and isothermal fatigue tests were conducted in closed-loop, servo-hydraulic testing machines at Westmoreland Mechanical Laboratory, Youngstown, PA using an axial extensometer on cylindrical specimens (diameter of 0.3 in and gage length of 0.5 in) heated by a radiation furnace. Applicable ASTM standards were employed by both testing laboratories.

2.2 Experimental Procedures

The fatigue testing cycles were selected to simulate the most critical conditions expected in an exhaust system during engine start up, operational transients and shut down. Table 1 briefly describes the isothermal (HRSC), the bithermal out-of-phase plastic-plastic fatigue (HROP), and the bithermal plastic-creep fatigue (CCOP) tests conducted in this study. See Ref. [4-6] for greater details on bithermal fatigue testing. Tests were conducted at various strainranges. The testing temperatures were selected based on considerations that the maximum service temperature was 800°C, and 400 °C was low enough to avoid creeping and hence only plastic

inelasticity was possible. Although the service condition goes to ambient temperatures (normally −30 to +40 °C), laboratory-testing time per cycle would be prohibitively long if the specimen had to be cooled to such low temperatures. The low temperature at 400°C still required 3 to 4 minutes to complete a cycle. For high-rate straining, an effective frequency of 0.5 was used (excluding the time to change temperature). High-rate strain cycling was used to preclude detectable creep deformation. During the time when the specimen temperature was changed uniformly from maximum to minimum, and vice versa, the axial load was controlled at zero. This precluded imposition of mechanical strain. Once the temperature had stabilized at the desired level, the appropriate loading (straining) was applied to achieve the desired type of inelastic strain (plasticity or creep).

For both out-of-phase HROP (PP) and CCOP (PC) tests, the tensile plastic deformation (P) is applied at the minimum temperature of 400°C until the prescribed strain limit is reached. Compressive plastic deformation (P) is applied at the maximum temperature only for the HROP tests. For the out-of-phase CCOP (PC) tests, the tensile plastic deformation (P) is applied at the minimum temperatures until the prescribed strain limit is reached. At that point, the direction of straining is reversed and the load is dropped rapidly to zero. Then the load is held at zero while the temperature is increased to the maximum. Following temperature stabilization, the temperature is held constant while a compressive stress is applied rapidly and held constant. In general some small compressive plasticity may occur upon application of the constant compressive creep stress. Compressive creep deformation (C) occurs with time until a prescribed total compressive strain limit has been reached. At this point, the load is rapidly decreased to zero. Under zero load control, the temperature is decreased to the minimum and the tensile plastic deformation is applied again. Completely reversed, high-rate, strain-controlled isothermal

fatigue tests (HRSC) were also performed at the same temperatures used in the bithermal tests (400 and 800°C).

III. Results and Discussion

Tensile, isothermal, bithermal and thermomechanical fatigue test results for SS409 for implementing the TS-SRP approach for exhaust systems are documented in this paper. Tensile tests were conducted at both 400 and 800°C. Values of elastic modulus, yield strength, ultimate strength, area reduction and elongation are given in Table 2.

3.1 Cyclic Failure Resistance

Fatigue failure lives of the PC cycles ranged from about 500 up to nearly 10,000 cycles corresponding, respectively, to the total strainranges from 0.820 % to 0.156 %. Creep hold periods in these tests covered only up to 2 minutes. The fatigue lives of the PP cycles covered from about 500 up to nearly 4000 cycles corresponding, respectively, to the total strainranges from 0.985 % to 0.203 %. Figure 2 displays these results. The small insert hysteresis loops schematically illustrate the bithermal out-of-phase cycles.

It is seen from Figure 2b that there is virtually no influence of the test type (PP or PC) on the cyclic life when compared at equal inelastic strainranges. The inelastic failure lines show relatively steep slopes and high fatigue ductility coefficients. The high coefficient is expected

since SS409 is a highly ductile alloy with an elongation of 94.3% and a reduction in area of 97.9% at 800°C (Table 2).

The PC elastic strainrange versus life relationship lies below the corresponding PP elastic line (Figure 2c). This is expected because more time is spent at the compressive high temperature in the PC bithermal tests, resulting in lower stresses corresponding to lower elastic strains. It is expected that PC cycles will be more detrimental that PP cycles at lower, nominally elastic, strainrange levels, where constitutive creep effects (and perhaps oxidation interactions) become greater. It has been noted that the compressive creep stress levels of the PC cycles with a 2-minute hold period is approximate half of the 0.2% offset yield strength at 800°C, thus precluding measurable plasticity. The result is that the inelastic strainrange consists almost entirely of PC, i. e., F_{pc} in equation (9) (Figure 1) is nominally equal to *1.0*.

The total strainrange versus life plot of Figure 2a doesn't reveal a significant difference between the PP and PC behavior because the total strainrange is dominated by the large inelastic strainrange components that were already observed to by nearly coincident.

As shown in Figure 3, there is a significant difference between bithermal and isothermal fatigue resistance. Schematic stress-strain hysteresis loops are shown for isothermal and bithermal cycling. Bithermal out-of-phase cycling has a profoundly detrimental influence on the fatigue life of SS409. Lives are reduced by a factor of 5 (compared to 800°C) or 15 (compared to 400°C) at a total strainrange of approximately 0.3%. The fatigue life reductions caused by the out-of-phase cycling would be difficult to predict using isothermal fatigue modeling only.

The lower the total strainrange, the greater the differences in life, and isothermal fatigue lives decrease with increasing temperature. At the strainrange of approximately 0.3%, the fatigue

life at 800°C is only about 25% of that at 400°C. At this strainrange at 800°C, the stress levels are only 12% of that at 400°C.

3.2 Cyclic Constitutive Response

Bithermal out-of-phase PC constitutive tests of SS409 between 400 and 800°C under creep stress hold were conducted to characterize the cyclic stress-strain response to time at temperature. The hold-time per cycle of the constitutive tests ranged from 42 seconds up to 1.5 hours and the total strainrange covered approximately 0.2 to 1.0%. Bithermal strain cycles were applied only until a stable hysteresis loop was achieved (≈10 cycles). As it was also observed for the failure tests, the tensile stress peak (400°C) was significantly higher than the compressive peak (800°C). SS409 displayed cyclic strain-hardening behavior for all applied bithermal out-of-phase strain cycles.

Since the inelastic strainrange consists almost entirely of PC for the current tests, the inelastic strainrange fraction F_{pc} is independent of time and total strainrange, which means that $m = 0$, $\alpha = 0$, and $A' = 1.0$. Figure 4 presents cyclic elastic strainrange versus inelastic strainrange ("strain-strain") relations for both PP and PC cycles. The cyclic strain-strain coefficient K_{pc} is a function of both time and total strainrange.

During isothermal PP testing, SS409 exhibits cyclic strain-hardening behavior at 400°C, but cyclic strain-softening at 800°C. The stress-strain hysteresis loops were approximately symmetrical in tension and compression for all isothermal tests.

3.3 Observations of Tested Specimens

All cyclically failed specimens macroscopically exhibited transgranular-appearing fracture surfaces showing evidence of classical fatigue striations. Most, but not all, specimens exhibited multiple crack initiation sites; some of which would link before final fracturing into two pieces. Evidence of intergranular cracking, normally associated with creep damage, was conspicuously absent despite large amounts of creep deformation in the PC tests. Since the PC and the PP tests exhibited nearly identical inelastic strainrange versus fatigue life curves, one could hypothesize that the creep- and plasticity-deformation mechanisms did not differ appreciably. However, no metallographic evidence has been generated to substantiate this conjecture. Nor was there a quantifiable effect of different oxidation exposure times on the cyclic crack initiation lifetimes measured in the current test program. As noted, there was a significant detrimental effect of bithermal cycling on life compared to isothermal cycling. Specimens tested isothermally at 800°C spent the entire test time at temperature, whereas bithermally-cycled specimens spent only half the test time at 800°C. Yet the isothermal tests exhibited considerably longer cyclic lives. All isothermally- and bithermally-tested specimens involving 800°C showed extensive oxidation. The oxide was black in color, even on the fatigue-cracked surfaces. No attempts were made to quantitatively model the severity of oxidation. The above results do not point to either creep or oxidation *per se* as being the governing damaging mechanism for the cyclic life differences between isothermal and bithermal tests. These observations are entirely consistent with the TS-SRP equations that have been written based upon the test data generated in this study. Although separation of oxidation and creep-plasticity effects has been successfully accomplished [8] within the SRP framework, it has not been generally adopted. The SRP approach currently does not track damage specifically due to oxidation. Nevertheless, this seemingly crucial omission has not rendered the method from being able to correlate and predict

high-temperature creep-fatigue and thermomechanical fatigue behavior of a wide range of types of metals and alloys in air and vacuum [4,9] for a variety of engineering applications.

As will be shown in the following section, the only appreciable and quantifiable effect on the thermomechanical fatigue resistance of SS409 has been that of hold-time per cycle altering the elastic strainrange versus inelastic strainrange ("strain-strain") relationship. TS-SRP recognizes this influence as directly affecting the elastic strainrange versus life relationship in the low-strain, long-life regime that is of such great importance to industrial applications. This is a creep effect, but a constitutive cyclic stress-strain-time effect, and not a creep deformation damaging effect, i.e., intergranular creep induced cracking.

3.4. Calibration of the TS-SRP Equation Constants for SS409

The TS-SRP equations have been calibrated for SS409 for out-of-phase bithermal TMF cycling. A log-log linear regression of the bithermal PP and PC inelastic strainrange versus life data yielded the following expressions for equations (3) and (4).

$$\Delta\varepsilon_{pp} = 4.08(N_{pp})^{-1.01} \tag{11}$$

$$\Delta\varepsilon_{pc} = 3.08(N_{pc})^{-0.96} \tag{12}$$

A similar fit of the bithermal PP elastic strainrange versus life data yields

$$\Delta\varepsilon_{el,pp} = 0.0036(N_{pp})^{-0.17} \tag{13}$$

Evaluation of the constants in the above equations has required cyclic tests conducted to failure. The equations and their constants are thus referred to as *failure* equations and constants.

Because equations (11) and (12) have nearly identical exponents, and because parallel PP and PC life relations greatly simplify the subsequent life prediction calculations, the coefficient of equation (12) has been recomputed using the PP value of c (= −1.01). Hence,

$$\Delta\varepsilon_{pc} = 4.02(N_f)^{-1.01} \tag{14}$$

The small difference between the coefficients C_{pp} (= 4.08) and C_{pc} (= 4.02) indicates a negligible influence of compressive creep strain *per se* on the out-of-phase bithermal fatigue *failure* resistance of SS409.

The constants for the balance of the TS-SRP equations of current concern are determined from cyclic stress-strain (constitutive) results either run to failure or stopped short of failure. These are the so-called *constitutive* constants.

The cyclic stress-strain behavior for bithermal out-of-phase PP is expressed as a cyclic strain-strain curve, i.e., cyclic elastic strainrange versus inelastic strainrange. The value of n can be estimated from the PP failure results and the PP constitutive results. Performing a log-log regression of equation (8) reveals,

$$\Delta\varepsilon_{pp,el} = 0.0036(\Delta\varepsilon_{in})^{0.20} \tag{15}$$

Similarly, multiple regression of the data supporting equation (10) produces the following equation for the time-dependent variable K_{pc}.

$$K_{pc} = 0.00269(\Delta\varepsilon_{to})^{-0.029}(\delta t)^{-0.046} \tag{16}$$

Substituting this result into equation (7) gives the coefficient of the elastic strainrange versus cyclic life for out-of-phase cycling as a function of the hold-time and the total strainrange. The corresponding inelastic strainrange is equation (14). Hence, the total strainrange versus cyclic life relation is

$$\Delta\varepsilon_{to} = 0.00269(\Delta\varepsilon_{to})^{-0.029}(\delta t)^{-0.046}(N_f)^{-0.17} + 4.02(N_f)^{-1.01} \tag{17}$$

For a known total strainrange and hold-time per cycle, the cyclic life can be computed for any bithermal out-of-phase cycle with temperature extremes of 400 and 800°C.

Table 3 summarizes the isothermal and bithermal *failure* and *constitutive* constants of SS409 for the TS-SRP approach. Note that $F_{pc} \approx 1.0$ for all of the bithermal PC tests, and the equation constants for K_{pc} were found to be: $\alpha = -0.029$, $m = -0.046$, and $A' = 0.00269$. With $F_{pc} = 1.0$, only 10 constants extracted from the bithermal experiments were needed to back-calculate all of the bithermal fatigue lives.

The software package, "*TS-SRP/PACK (LEW-15653)*♣," was used to process the data and calculate thermomechanical (bithermal) fatigue lives in this investigation. Correlation between predicted and observed lives is given in Table 4. A general introduction to the Total Strain Version of Strainrange Partitioning (TS-SRP) approach, and instruction on how to use the software are given in Refs. [10,11].

♣ *Computer Software Management and Information Center* (COSMIC), current address is: University Corporation for Atmospheric Research, COSMIC Program, Boulder, CO 80307

Equation (17) was used to calculate the fatigue lives of all of the bithermal out-of-phase tests performed herein a 400 and 800°C. A comparison of the calculated versus observed lives are presented in Table 4 and Figure 5. Life predictions were performed over the range of data, which were used to establish the life relations of the TS-SRP approach. The calculated fatigue lives are in very good agreement with the observed lives. The TS-SRP approach correlated 70% of the data within a factor of 1.2 of the observed lives, 85% of the data within a factor of 1.4 and 100% of the data within a factor of 1.8.

IV. Summary and Conclusions

1. The Total Strain Version of Strainrange Partitioning (TS-SRP) was evaluated for the ferritic stainless steel alloy SS409 used extensively in automotive exhaust systems. Thermomechanical, out-of-phase, cyclic *failure* and *constitutive* behaviors were measured for bithermal tests cycling between isothermal extremes of 400 and 800°C. Fatigue lives covered up to 10,000 cycles to failure for hold-times per cycle of up to 2.0 minutes. Cyclic constitutive hold-time tests, not run to failure because of prohibitively long testing times, covered up to 1.5 hours per cycle. For all hold-time tests, the PC strainrange was nearly 100% of the measured inelastic strainrange.

2. On an inelastic strainrange basis, there was a negligibly small influence on cyclic life of the type (PP or PC) of out-of-phase bithermal test. Both PP and PC inelastic failure lines were nearly identical. Both showed a very high fatigue ductility coefficient (≈4.0) and steep slope (≈-1.0).

3. On a total strainrange basis and at low strainranges, PC type cycles are more detrimental that PP. In this regime, the creep constitutive behavior was observed to exert a significant influence on the cyclic stress-strain response, which the TS-SRP life prediction method translates into an implied strong detrimental influence on cyclic life.

4. The bithermal fatigue behavior was compared to completely reversed, strain-controlled, isothermal fatigue behavior at 400 and 800°C. Bithermal out-of-phase cycling between 400 and 800°C had a profound detrimental influence on fatigue life (factors of 15 and 5 less, respectively, than 400 and 800°C isothermal lives). The investigation confirmed the inadvisability of using an isothermal fatigue database and model for designing and lifing of automotive exhaust systems.

5. To assess the ability of the TS-SRP method to correlate results, it was used to back-calculate the cyclic lives for all of the bithermal creep-fatigue tests. The approach was found to

correlate 70% of the data within a factor of 1.2 on life, 85% of the data within a factor of 1.4 and 100% of the data within a factor of 1.8. The results reflect an acceptably high fidelity of correlatability for the TS-SRP approach for the intended application.

Acknowledgment

The authors are grateful to Mr. John M. Grace and Mr. Robert T. Usleman at Arvin Industries, Inc. for their encouragement and financial support.

References

1. Anon (1997) Thermal and Thermomechanical Fatigue of Structural Alloys, *Heat-Resistant Materials*, ASM Specialty Handbook, J. R. Davis, Ed., 527-556.

2. G. R. Halford (1987) Low-Cycle Thermal Fatigue (Chapter 6) In: R. B. Hetnarski, Ed., *Thermal Stresses II.* Elsevier, Amsterdam.

3. D. A. Miller, R. H. Priest and E. G. Ellison (1984) A Review of Material Response and Life Prediction Techniques under Fatigue-Creep Loading Conditions. In: *High Temperature Materials and Processes*, 6, 155-194.

4. G. R. Halford, M. A. McGaw, R. C. Bill, and P. D. Fanti (1988) Bithermal Fatigue: A Link Between Isothermal and Thermomechanical Fatigue. *Low Cycle Fatigue*, ASTM STP 942, H. D.

Solomon, G. R. Halford L. R. Kaisand, and B. N. Leis, Eds., American Society for Testing and Materials, Philadelphia, pp. 625-637.

5. J. F. Saltsman and G. R. Halford (1988) Life Prediction of Thermomechanical Fatigue Using The Total Strain Version of Strainrange Partitioning (SRP)---A Proposal. NASA TP-2779, February.

6. G. R. Halford, M. J. Verrilli, S. Kalluri, F. J. Ritzert, R. E. Duckert (1992), and F. A. Holland, "Thermomechanical and Bithermal Fatigue Behavior of Cast B1900+Hf and Wrought Haynes 188," *Advances in Fatigue Lifetime Predictive Techniques, ASTM STP-1122*, M. R. Mitchell and R. W. Landgraf, Eds. , American Society for Testing and Materials, Philadelphia, pp. 120—142.

7. J. F. Saltsman and G. R. Halford (1989), Procedures for Characterizing an Alloy & Predicting Cyclic Life Using the Updated Total Strain Version of Strainrange Partitioning. NASA TM-4102, June.

8. S. Kalluri, S. S. Manson, and G. R. Halford (1987), "Exposure Time Considerations in High Temperature Low Cycle Fatigue," *Proceedings, Fifth International Conference on Mechanical Behavior of Materials (ICM-5, Beijing)*, M. G. Yan, S. H. Zhang, and Z. M. Zheng, Eds., Pergamon Press, Vol. 2, pp. 1029-1036.

9. Anon. (1978), AGARD Conference on Characterization of Low Cycle High Temperature Fatigue by the Strainrange Partitioning Method, AGARD CP-243, Aalborg, Denmark

10. J. F. Saltsman (1989), "Computer Programs to Characterize Alloys and Predict Cyclic Life Using the Total Strain Version of Strainrange Partitioning—Tutorial and Users Manual," COSMIC Program # LEW-15653, Volume 1 of 2, *Computer Software Management and Information Center* (COSMIC), Athens, GA 30602-4272.

11. J. F. Saltsman (1989), " Procedures for Characterizing an Alloy and Predicting Cyclic Life With the Total Strain Version of Strainrange Partitioning," COSMIC Program # LEW-15653, Volume 2 of 2, *Computer Software Management and Information Center* (COSMIC), Athens, GA 30602-4272.

LIST OF TABLES

LIST OF FIGURES

Table 1. Summary of test types and conditions

Test type	Temp. (°C)
Tensile test [#]	400
	800
HRSC—Isothermal, high-rate, continuous strain cycle producing 100% PP strainrange [#]	400
	800
HROP—Bithermal, out-of-phase, high-rate, strain cycle producing 100% PP strainrange [†]	400 ⇔ 800
CCOP—Bithermal, out-of-phase, compressive creep, tensile plasticity cycle producing PP and PC strainranges [†]	400 ⇔ 800

#: Conducted at Westmoreland Mechanical Testing & Research Inc., Old Rt.30, Westmoreland Drive, Youngstown, PA 15696
†: Conducted at Mar-Test Inc., 1245 Hillsmith Drive, Cincinnati, OH 45215

Table 2. Tensile mechanical properties of SS409

Temp. (°C)	Ultimate Tensile Strength, UTS (MPa)	Yield Strength, 0.2 % YS (MPa)	Elongation (%)	Reduction of Area, %RA	True Ductility, D§	Elastic Modulus, E (GPa)	UTS/E
400	256	120	35.7	85.4	1.92	172	0.001488
800	31	22	94.3	97.9	3.86	117	0.000265

§: True Ductility, D = ln[100/(100−%RA)]
‡: interpolated values

Table 3. Coefficients *failure* and *constitutive* constants of SS409 for TS-SRP

Temp. (°C)	Coefficients			Exponents		
	C	*B*	*K*	*c*	*b*	*n*
	Bithermal out-of-phase plastic-plastic fatigue (HROP)					
400 ⇔ 800	4.08	0.0036	0.0033	–1.01	–0.174	0.200
	Bithermal out-of-phase plastic-creep fatigue (CCOP)					
400 ⇔ 800	4.02	------	-----	–1.01	------	-----
	Isothermal plastic-plastic fatigue (HRSC)					
400	2.13	0.0035	0.0030	–0.74	–0.051	0.048
800	2.26	0.0017	0.0010	–0.73	–0.160	0.175

Table 4. Correlation of calculated and observed bithermal out-of-phase fatigue lives of SS409, 400 ⇔ 800 °C

Spec. No.	Test type	Bithermal Temps. (°C)	Hold time /cycle, δt (minutes)	Observed life (cycles)	Calculated life (using Eq. 17) (cycles)	Calculated (using Eq. 17) /Observed
BF4	PP	400 ⇔ 800	0	529	454	0.858
BF9	PP	400 ⇔ 800	0	586	639	1.090
BF5	PP	400 ⇔ 800	0	1148	1026	0.894
BF7	PP	400 ⇔ 800	0	1266	2237	1.767
BF10	PP	400 ⇔ 800	0	1743	2359	1.353
BF12	PP	400 ⇔ 800	0	2857	3938	1.378
BF15	PP	400 ⇔ 800	0	3819	4435	1.161
BF3	PC	400 ⇔ 800	1.67	520	512	0.985
BF6	PC	400 ⇔ 800	1.67	1066	898	0.842
BF11	PC	400 ⇔ 800	0.70	1848	2099	1.136
BF8	PC	400 ⇔ 800	1.83	2558	2353	0.920
BF13	PC	400 ⇔ 800	1.50	2966	2834	0.955
BF17	PC	400 ⇔ 800	1.00	9429	15782	1.674

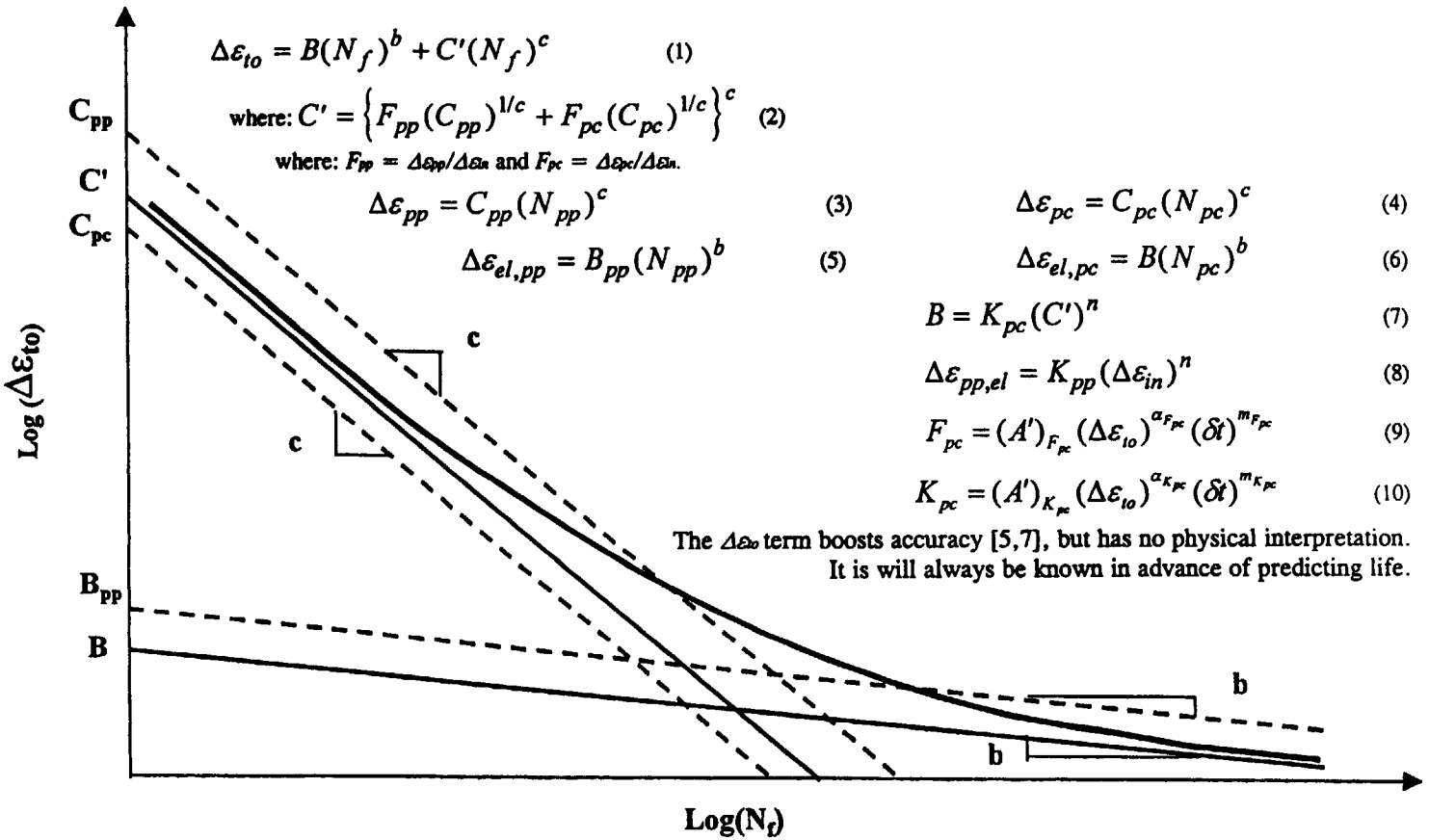
$\Delta\varepsilon_{to} = B(N_f)^b + C'(N_f)^c$ (1)
where: $C' = \left\{F_{pp}(C_{pp})^{1/c} + F_{pc}(C_{pc})^{1/c}\right\}^c$ (2)
where: $F_{pp} = \Delta\varepsilon_{pp}/\Delta\varepsilon_{in}$ and $F_{pc} = \Delta\varepsilon_{pc}/\Delta\varepsilon_{in}$.
$\Delta\varepsilon_{pp} = C_{pp}(N_{pp})^c$ (3)
$\Delta\varepsilon_{pc} = C_{pc}(N_{pc})^c$ (4)
$\Delta\varepsilon_{el,pp} = B_{pp}(N_{pp})^b$ (5)
$\Delta\varepsilon_{el,pc} = B(N_{pc})^b$ (6)
$B = K_{pc}(C')^n$ (7)
$\Delta\varepsilon_{pp,el} = K_{pp}(\Delta\varepsilon_{in})^n$ (8)
$F_{pc} = (A')_{F_{pc}}(\Delta\varepsilon_{to})^{\alpha_{F_{pc}}}(\delta t)^{m_{F_{pc}}}$ (9)
$K_{pc} = (A')_{K_{pc}}(\Delta\varepsilon_{to})^{\alpha_{K_{pc}}}(\delta t)^{m_{K_{pc}}}$ (10)
The $\Delta\varepsilon_{to}$ term boosts accuracy [5,7], but has no physical interpretation.
It is will always be known in advance of predicting life.
C_{pp}
C'
C_{pc}
B_{pp}
B
c
c
b
b
Log ($\Delta\varepsilon_{to}$)
Log(N_f)

Fig. 1

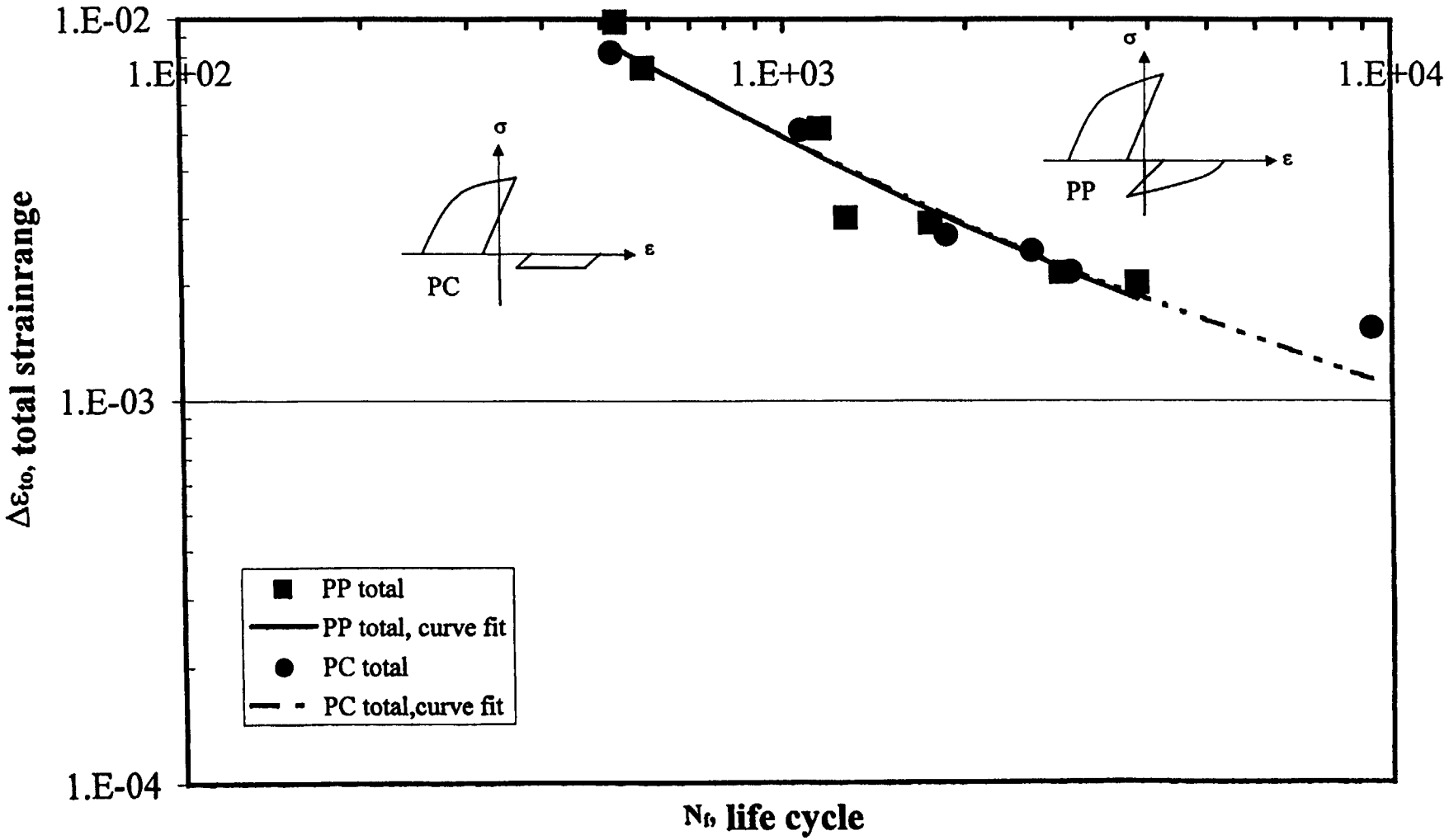
1.E-02
1.E-03
1.E-04
1.E+02
1.E+03
1.E+04
$\Delta\varepsilon_{to}$, total strainrange
N_f, life cycle
σ
ε
PC
σ
ε
PP
PP total
PP total, curve fit
PC total
PC total,curve fit

Fig. 2(a)

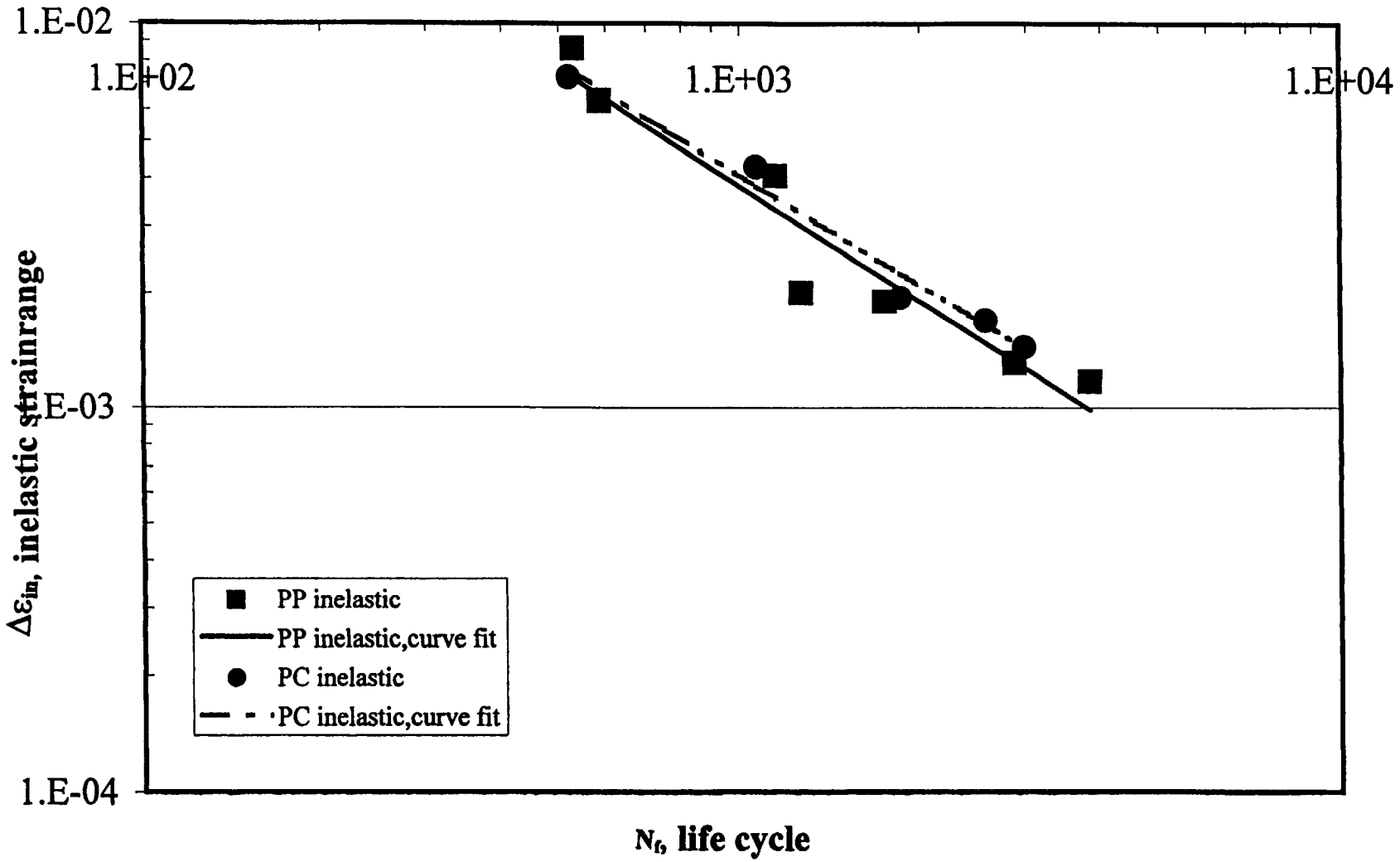
1.E-02
1.E+02
1.E+03
1.E+04
E-03
1.E-04
Δε_in, inelastic strainrange
N_f, life cycle
PP inelastic
PP inelastic,curve fit
PC inelastic
PC inelastic,curve fit

Fig. 2(b)

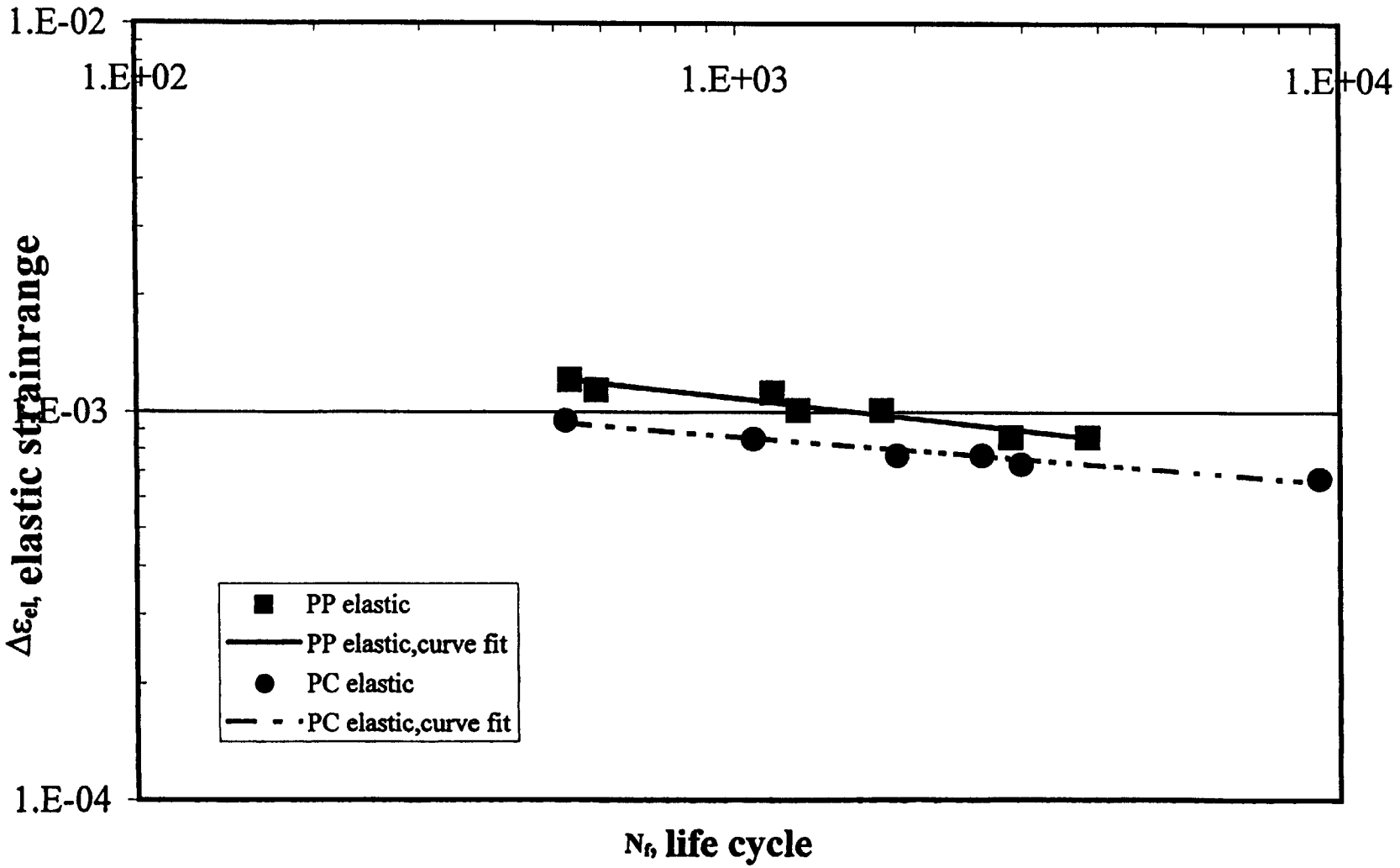
1.E-02
1.E+02
1.E+03
1.E+04
E-03
1.E-04
$\Delta\varepsilon_{el}$, elastic strainrange
N_f, life cycle
PP elastic
PP elastic,curve fit
PC elastic
PC elastic,curve fit

Fig. 2(c)

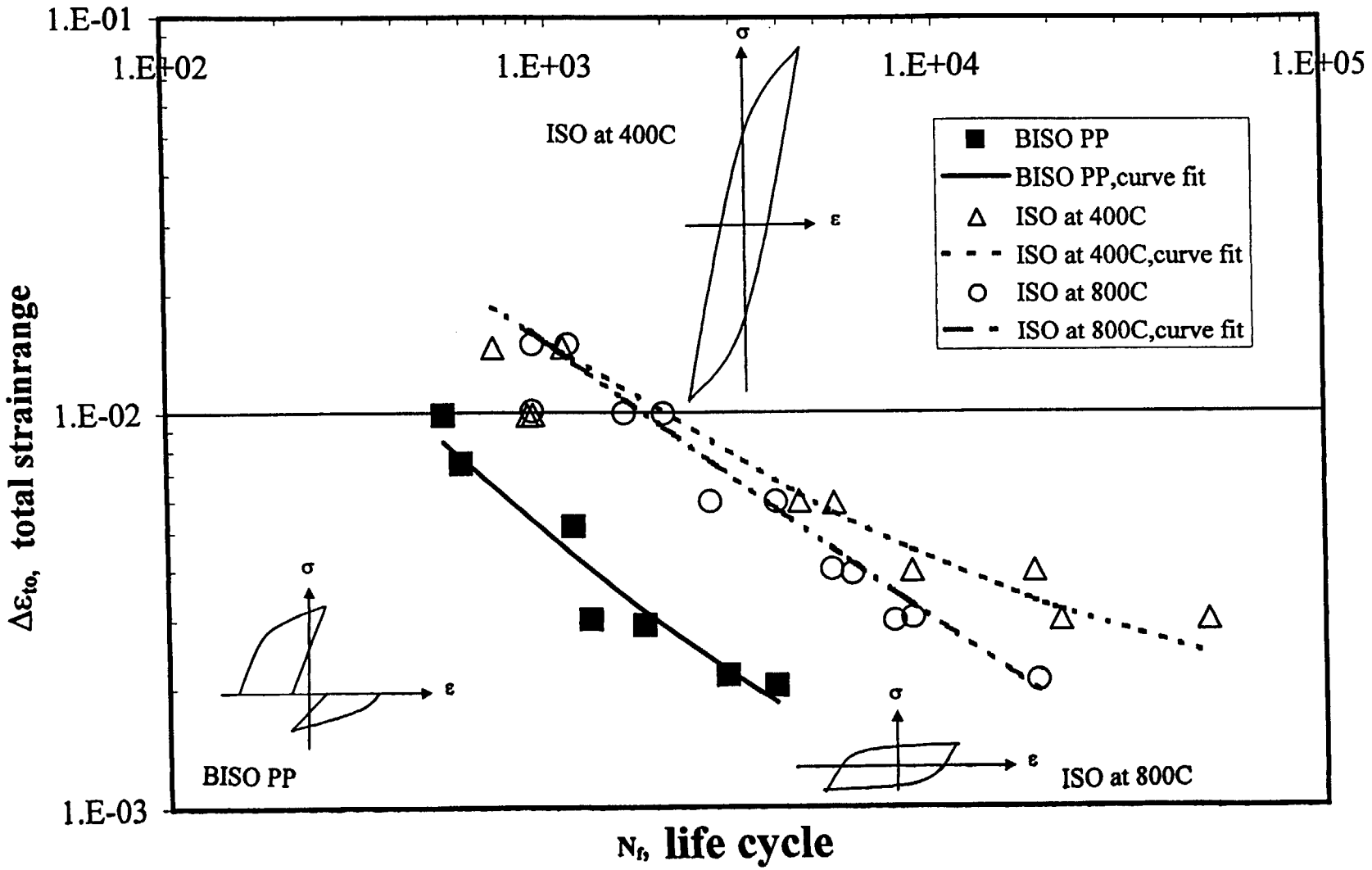
1.E-01
1.E+02
1.E+03
1.E+04
1.E+05
1.E-02
1.E-03
$\Delta\varepsilon_{to}$, total strainrange
N_f, life cycle
ISO at 400C
BISO PP
ISO at 800C
σ
ε
BISO PP
BISO PP,curve fit
ISO at 400C
ISO at 400C,curve fit
ISO at 800C
ISO at 800C,curve fit

Fig. 3

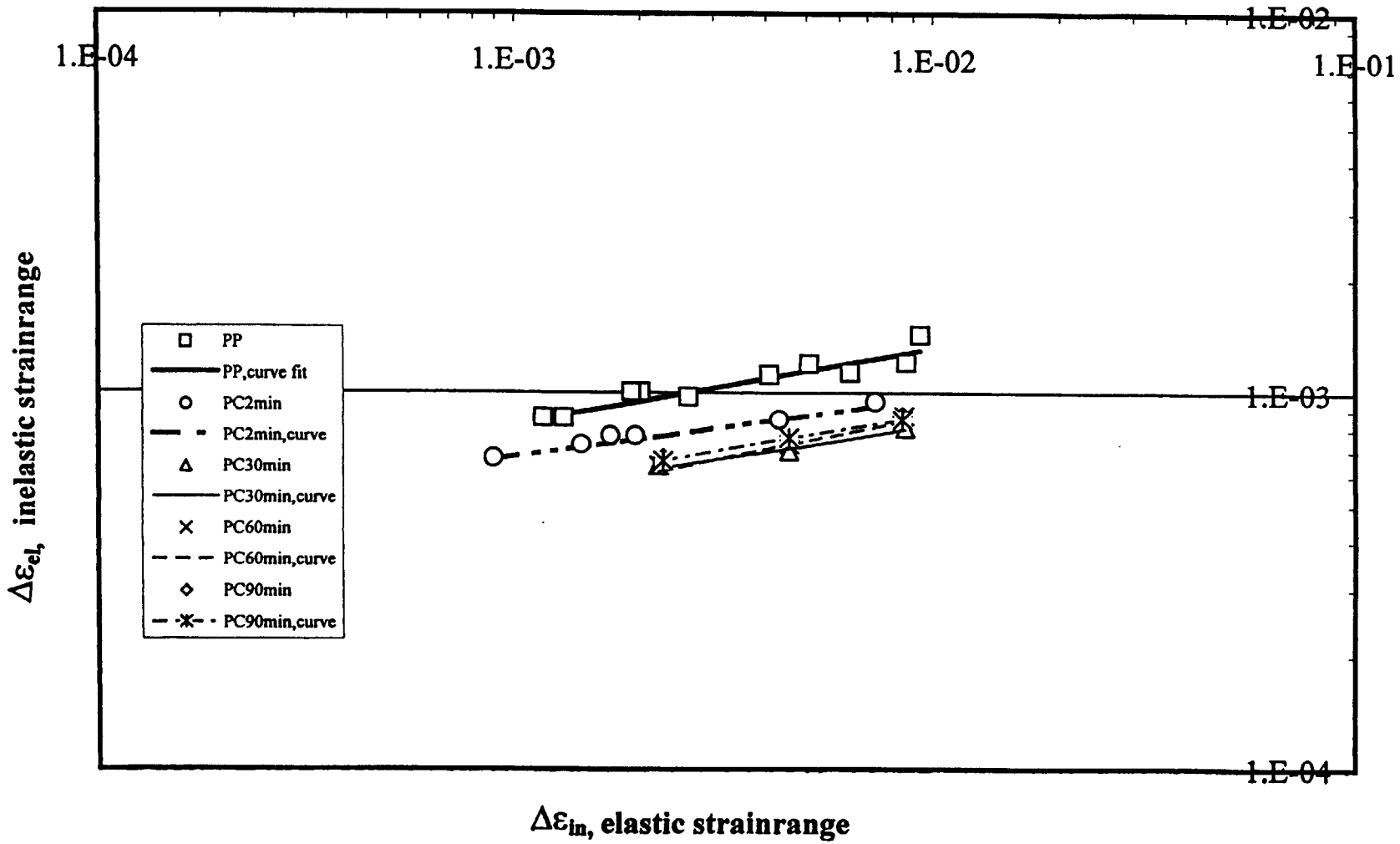
1.E-04
1.E-03
1.E-02
1.E-01
1.E-02
1.E-03
1.E-04
PP
PP,curve fit
PC2min
PC2min,curve
PC30min
PC30min,curve
PC60min
PC60min,curve
PC90min
PC90min,curve
Δεel, inelastic strainrange
Δεin, elastic strainrange

Fig. 4

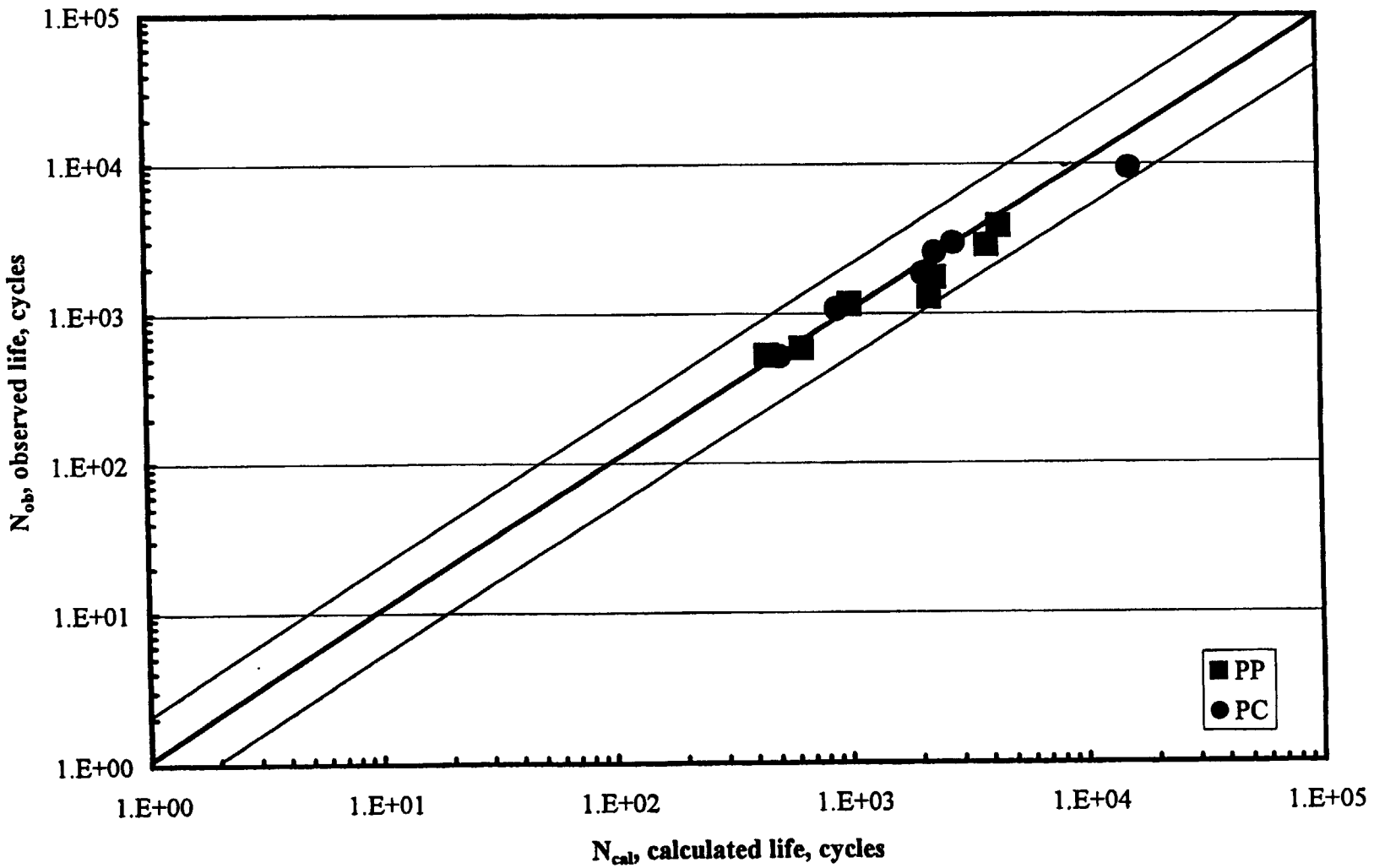
1.E+05
1.E+04
1.E+03
1.E+02
1.E+01
1.E+00
N_{ob}, observed life, cycles
1.E+00
1.E+01
1.E+02
1.E+03
1.E+04
1.E+05
N_{cal}, calculated life, cycles
PP
PC

Fig. 5